Electronic Supplementary Material (ESI) for Materials Horizons.

Supporting Information

Spatial Exciton Allocation Strategy with Reduced Energy Loss for High-Efficiency Fluorescent/Phosphorescent Hybrid White Organic Light-Emitting Diodes

Fangchao Zhao, Ying Wei, Hui Xu, Dustin Chen,Tansir Ahamad, Saad Alshehri, Qibing Pei and Dongge Ma**

Monte-Carlo simulation of exciton migration in doping systems

Exciton migration process was portrayed with Monte-Carlo method, performed with C+ language and visualized with MATLAB software package.

Two models were established to describe the different exciton migration processes in the doping systems without or with exciton traps, corresponding to NPB:PO-01 and TAPC:PO-01 systems, respectively. A matrix was firstly constructed with two kinds of points, representing host and dopant molecules. For the next step of exciton migration, the probabilities of these two points were 0.95 and 0.05, respectively, corresponding to host and dopant concentrations. The situation of NPB:PO-01 can be simplified as: i) if present point is host, exciton can migrate with probability of 1 (case 1); ii) if present point is dopant, exciton can migrate or deexcitation with probability of 0.5 (case 2 and 3). While, for TAPC:PO-01, in the case of host as present point, exciton can migrate with probability of 1 (case 4); in the case of dopant as present point, i) if next point is host, exciton can deexcitation with probability of 1 (case 5); ii) if next point is dopant, exciton can migrate or deexcitation with probability of 0.5 (case 6 and case 7).

So, for NPB:PO-01 simulation, we generate a random number R(0,1) in the range of 0 to 1.

(1) If $0<R<0.05$, point is dopant; if $0.05<R<1$, point is host.

(2) If $0.05<R<1$, the migration went to case 1;

If $0<R<0.05$, another random number R'(0,1) between 0 and 1 was generated:

If $0<R'<0.5$, the migration went to case 2;

If $0.5<R'<1$, the migration went to case 3.

While, for TAPC:PO-01 simulation, two random number R1 and R2 were also generated firstly, corresponding to present and next points.

(1) If $0.05<R1<1$, the migration went to case 4;

(2) If $0<R1<0.05$ and $0.05<R2<1$, the migration went to case 5;

If $0<R1,R2<0.05$, another random number R'(0,1) between 0 and 1 was generated:

If $0<R'<0.5$, the migration went to case 6;

If $0.5<R'<1$, the migration went to case 7.

Then, a random-walk model was adopted to define exciton migration process. On account of space symmetry and migration randomness, the migration process in 3D space can be simplified to two dimensions in a form of grid, in which each molecule is a nodal point with coordinates of (x, y). In this case, exciton migration process can correspond to coordinates of the finally located molecule. We assumed that exciton can migrate to the nearest neighboring molecule. Therefore, when setting the starting point at (0, 0), each migration step rendered the 1 unit variation of coordinates. Taking account of random migration for each step, coordinate variation at each step, D, can be:

$$D = \begin{cases} (1, 0) & \text{case 8 with 1/4 probability} \\ (-1, 0) & \text{case 9 with 1/4 probability} \\ (0, 1) & \text{case 10 with 1/4 probability} \\ (0, -1) & \text{case 11 with 1/4 probability} \end{cases}$$

Then, the final location of exciton after N steps is $\sum_{1}^{N} \Delta$.

The criteria for exciton migration were defined:

(1) For each step, we generate a random number R''(0,1) in the range of 0 to 1.

If 0< R"(0,1)<1/4 the migration goes to case 8;

If 1/4< R"(0,1)<1/2 the migration goes to case 9;

If 1/2< R"(0,1)<3/4 the migration goes to case 10;

If 3/4< R"(0,1)<1 the migration goes to case 11;

(2) If not terminated by case 3, 5 and 7, migration can continue for 5000 steps. No matter early termination or not, the final exciton location was recorded.

(3) The simulation was repeated for 10^6 times for each system to obtain big enough datasets for statistics and better approximate actual situations.

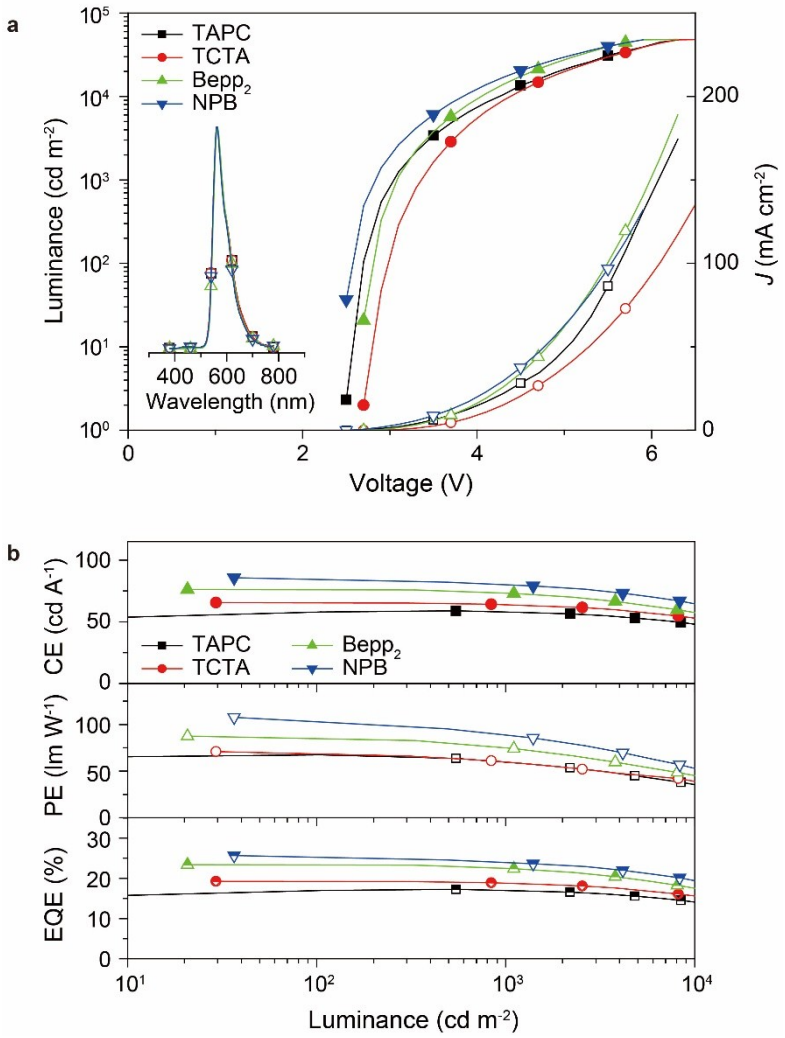

Fig. S1. EL performance of yellow PHOLEDs based on various host materials with configuration of ITO/MoO_3 (8 nm)/NPB (60 nm)/TAPC (5 nm)/**Host**: PO-01 (5wt%, 10 nm)/$Bepp_2$ (30 nm)/LiF (1 nm)/Al (100 nm). **a.** Luminance-*J*-Voltage curves and EL spectra (inset); **b.** Efficiency-Luminance curves.

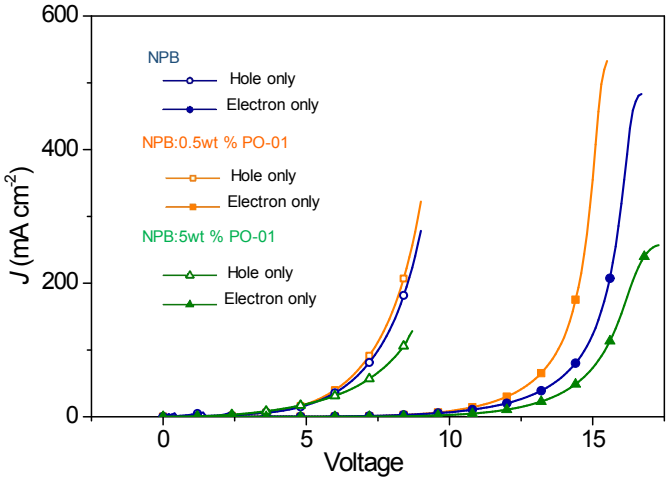

Fig. S2. *J-V* characteristics of single-carrier only devices of neat NPB and PO-01 doped NPB. For electron-only and hole-only devices, the configurations are ITO/LiF(1nm)/$Bepp_2$(40nm)/EML(40nm)/$Bepp_2$(40nm)/LiF(1nm)/Al and ITO/MoO_3(8nm)/NPB(40nm)/EML(40nm)/NPB(40nm)/MoO_3(8nm)/Al, respectively.

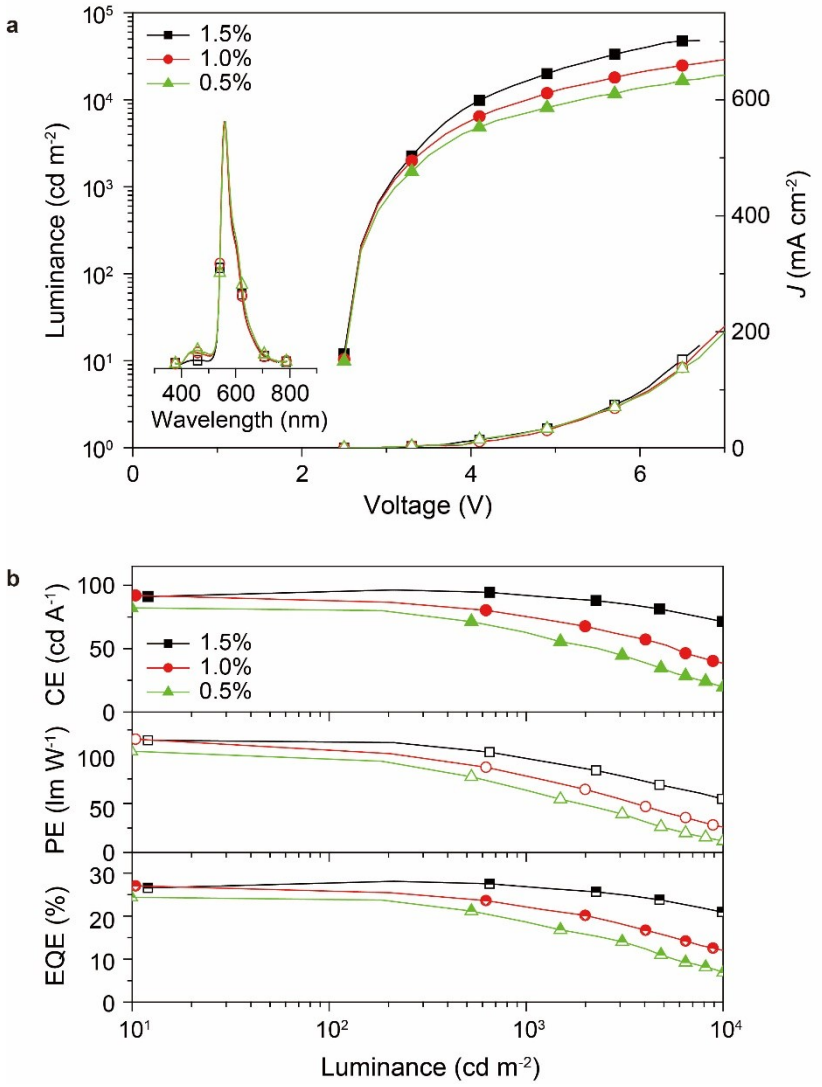

Fig. S3. EL performance of NPB-based PHOLEDs with **Device I** configuration and different PO-01 doping concentrations. **a.** Luminance-*J*-Voltage curves and EL spectra (inset); **b.** Efficiency-Luminance curves.

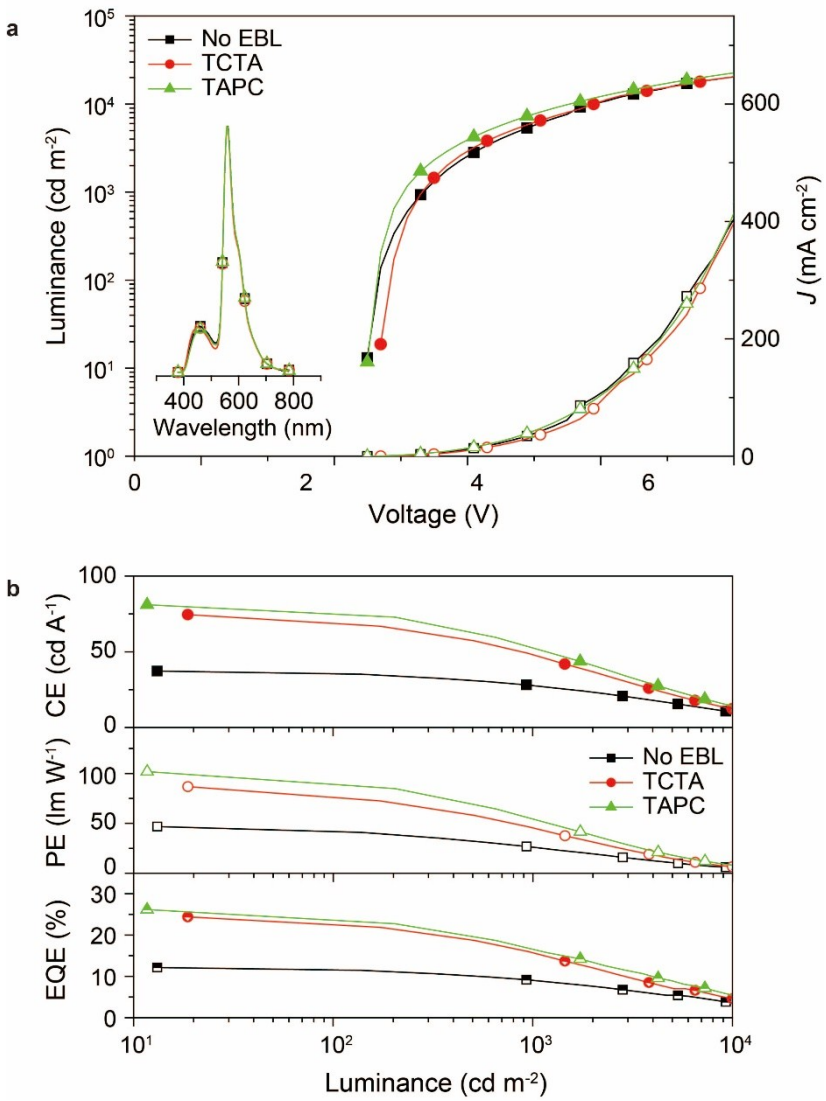

Fig. S4. EL performance of **Device II** type devices without or with different exciton blocking layers (EBL). **a.** Luminance-*J*-Voltage curves and EL spectra (inset); **b.** Efficiency-Luminance curves.

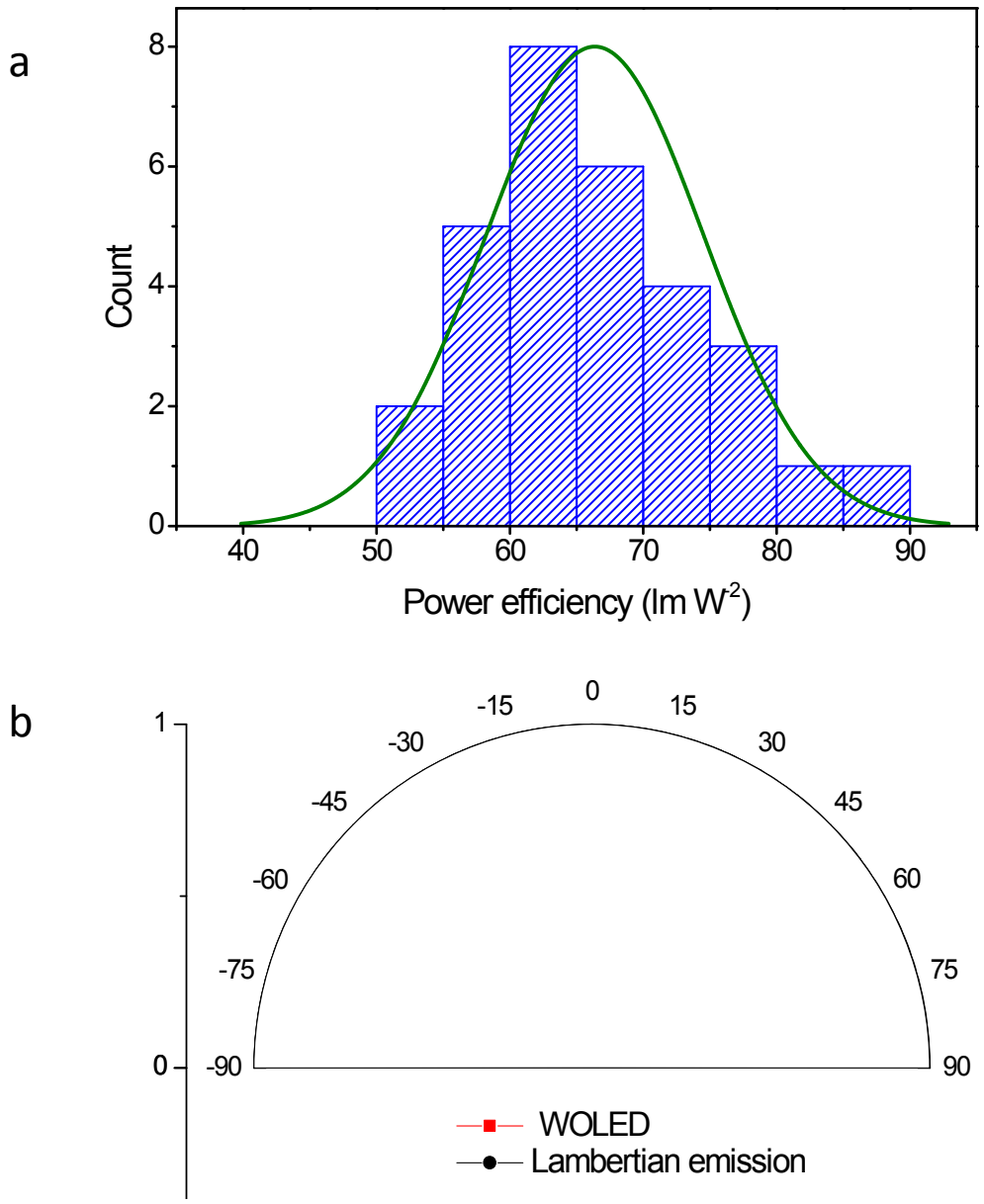

Fig. S5 a. Histogram of power efficiencies of Device II measured from 30 devices; **b.** Angular distribution of the luminance of Device II at 1000 cd m^{-2} (red) and typical Lambertian emission curve (black).

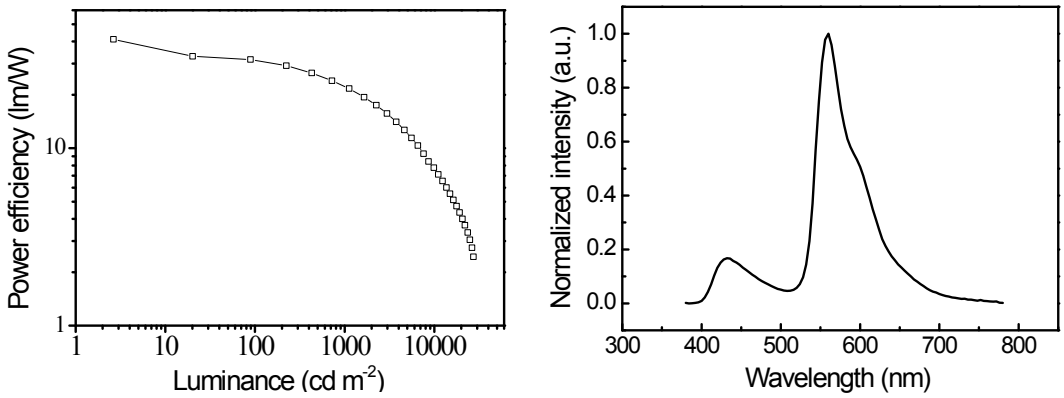

Fig. S6. Power efficiency and EL spectra at 1000 cd m^{-2} with structure of ITO/MoO_3 (8 nm)/NPB (60 nm)/TAPC (5 nm)/**NPB**:PO-01 (5%, 5 nm)/NPB (10 nm)/TPBI (30 nm)/LiF (1 nm)/Al (100 nm).

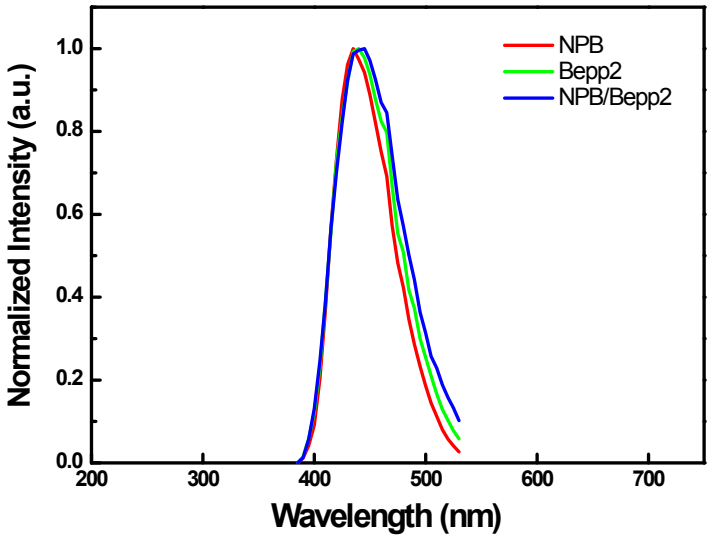

Fig. S7. PL spectrum of NPB film, Bepp2 film and NPB/Bepp2 bilayer film.

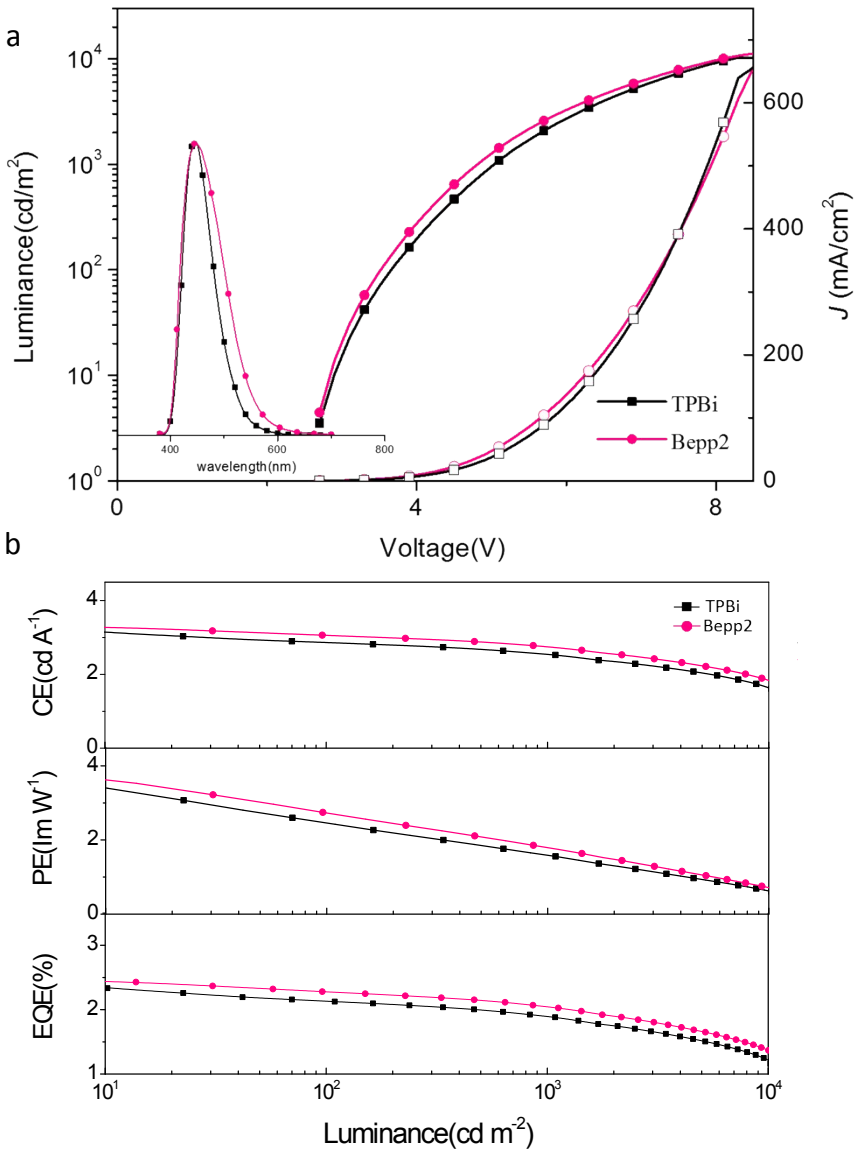

Fig. S8 Luminance-J-Voltage curves (a) and EL spectra (inset) and Efficiency-Luminance curves (b) of blue device with structure of ITO/MoO3 (8 nm)/NPB (60 nm)/TAPC (5 nm)/NPB (15 nm)/ETL (30 nm)/LiF (1 nm)/Al (100 nm).